Femtosecond Pump-Probe Spectroscopy of Conjugated Polymers: Coherent and Sequential Contributions

W. B. Bosma and S. Mukamel
Department of Chemistry, University of Rochester, Rochester, New York 14627
B. I. Greene
AT&T Bell Laboratories, Murray Hill, New Jersey 07974
S. Schmitt-Rink
Department of Physics and Materials Sciences Center, Philipps University, 3550 Marburg, Federal Republic of Germany
(Received 9 October 1991)

We report femtosecond pump-probe difference absorption experiments on polydiacetylene-*para*-toluene sulfonate. Theoretical analysis using a three-mode Brownian oscillator model for the nuclear dynamics reveals spectral diffusion in this conjugated polymer; this effect cannot be accounted for using the optical Bloch equations. Sequential (pump first) time ordering is dominant for resonant excitation, whereas experiments utilizing an off-resonant pump are dominated by nonsequential time orderings of the pump and the probe; the latter represent coherent (Raman-type) processes.

PACS numbers: 61.41.+e, 42.65.Dr

Polydiacetylene-*para*-toulene sulfonate (PTS) is a model one-dimensional semiconductor, characterized by a strong excitonic transition and a large third-order nonlinear optical susceptibility [1–5]. Previous pump-probe and stimulated Raman studies of PTS were interpreted using a phase-space filling model [3] for resonant excitation and the "phonon-mediated optical Stark effect" [4,6] for nonresonant excitation. While the former theory realistically models the excitonic response in the absence of phonons, the latter theory includes phonon effects, but is limited to nonresonant excitation. In this Letter, we report a series of resonant and off-resonant pump-probe experiments on PTS which reveal picosecond spectral diffusion in this conjugated polymer. This effect is modeled quantitatively using a Brownian oscillator model [7], which also describes for the first time the detailed structure of both the resonant and nonresonant signals.

In the experiments reported here, a thin film of PTS (ca. 100 Å) at $T=300$ K is subjected to a spectrally narrow pump pulse, centered at time $t=-\tau$, and a broadband probe, centered at $t=0$. The pulses are both ~ 70 fs in duration. The transmitted probe is frequency dispersed using an optical multichannel analyzer. The probe difference absorption is measured as a function of the detection frequency (ω_T), for a given delay time (τ) and pump center frequency (Ω_p) [4].

The pump-probe signal can be analyzed using the nonlinear response function [7]. When the pump and probe pulses are weak, the relevant signal is fourth order in the applied fields. We assume that the pump pulse is long compared to the inverse absorption linewidth and that the probe pulse is infinitely short [8]. We further assume that the PTS crystal has two experimentally relevant electronic states (the crystal ground state and an excitonic state, see Fig. 1), and that the dipole operator for the transition between those states is independent of the nuclear coordinates (the Condon approximation). We may then write the pump-probe difference absorption signal as [7,9]

$$S_{\rm tot}(\Omega_p,\omega_T;\tau)=S_p(\Omega_p,\omega_T;\tau)+S_c(\Omega_p,\omega_T;\tau)\,,$$

where

$$S_s(\Omega_p,\omega_T;\tau)=2\,\mathrm{Re}\sum_{a,b,c,d}P(a)\mu_{ab}\mu_{bc}\mu_{cd}\mu_{da}\int_0^\infty dt_2\,E_p(\tau-t_2)E_p^*(\tau-t_2)$$
$$\times\{e^{-i\omega_{db}t_2}\hat{R}_1(\omega_{dc}-\omega_T,t_2,\Omega_p-\omega_{da})+e^{-i\omega_{db}t_2}\hat{R}_2(\omega_{dc}-\omega_T,t_2,\Omega_p-\omega_{ba})$$
$$+e^{-i\omega_{ac}t_2}\hat{R}_3(\omega_T-\omega_{dc},t_2,\Omega_p-\omega_{ba})+e^{-i\omega_{ca}t_2}\hat{R}_4(\omega_T-\omega_{ba},t_2,\Omega_p-\omega_{da})\}\,, \tag{1a}$$

$$S_c(\Omega_p,\omega_T;\tau)=2\,\mathrm{Re}\sum_{a,b,c,d}P(a)\mu_{ab}\mu_{bc}\mu_{cd}\mu_{da}\int_0^\infty dt_2\,E_p^*(\tau)E_p(\tau+t_2)e^{i(\omega_T-\Omega_p)t_2}$$
$$\times\{e^{-i\omega_{db}t_2}\hat{R}_1(\omega_{dc}-\omega_T,t_2,\omega_T-\omega_{da})+e^{-i\omega_{db}t_2}\hat{R}_2(\omega_{dc}-\omega_T,t_2,\Omega_p-\omega_{ba})$$
$$+e^{-i\omega_{ac}t_2}\hat{R}_3(\omega_T-\omega_{dc},t_2,\Omega_p-\omega_{ba})+e^{-i\omega_{ca}t_2}\hat{R}_4(\omega_T-\omega_{dc},t_2,\omega_T-\omega_{da})\}\,. \tag{1b}$$

Equations (1) allow us to consider some of the relevant nuclear modes of the system in the vibronic eigenstate representation and some modes in the coordinate representation. The indices $a,c,\ldots$ and $b,d,\ldots$ in Eqs. (1) are summed over the vibronic eigenstates of the ground and excited states, respectively, of those modes which are considered in the vibronic eigenstate representation (Fig. 1). $\hbar\omega_{\nu\lambda}\equiv E_\nu-E_\lambda$ is the energy of the $\nu\rightarrow\lambda$ transition, and $\mu_{\nu\lambda}$ is the corresponding Franck-Condon overlap. $E_p(t)$ is the pump pulse temporal envelope. $P(a)$ is the probability to be in state $|a\rangle$ at thermal equilibrium, and Re denotes the real part. The functions $\hat{R}_j(\omega_3,t_2,\omega_1)$ are given by

$$\hat{R}_j(\omega_3,t_2,\omega_1)=\int_0^\infty dt_1\int_0^\infty dt_3\exp(i\omega_1 t_1+i\omega_3 t_3)R_j(t_3,t_2,t_1),\quad j=1,\ldots,4, \tag{2}$$

where $R(t_3,t_2,t_1)=\sum_{j=1}^4 R_j(t_3,t_2,t_1)$ is the third-order nonlinear response function for those modes which are considered in the coordinate representation. The nonlinear response function is the sum of four Liouville-space pathways R_j (and their complex conjugates), which correspond to different bra and ket interactions of the density matrix with the laser fields [7]. If we perform the t_2 Fourier transform in Eqs. (1), we have response functions with three frequency arguments; a resonance in the signal is obtained when some or all of those frequencies are near zero.

The pump-probe signal requires two interactions with the pump pulse and two interactions with the probe (the last probe interaction is the detection). $S_s(\omega_T,\Omega_p;\tau)$ corresponds to the sequential time ordering of these interactions: pump-pump-probe-probe. It is the only term which survives when the pulses are well separated (large τ), and is thus the dominant term in time-resolved hole-burning experiments. The second term, S_c, represents the other two possible time orderings, namely, pump-probe-pump-probe and probe-pump-pump-probe. If the pump laser is tuned below the zero-phonon to zero-phonon transition ($\Omega_p<\omega_{eg}$), the first ($\hat{R}_1$) and fourth ($\hat{R}_4$) terms of S_c dominate the signal, which peaks when both ω_T and $\omega_T-\Omega_p$ are nearly resonant; S_c is thus the term describing time-resolved "inverse" Raman scattering experiments [10]. S_c furthermore describes the optical Stark effect to second order in the pump field. By varying Ω_p and τ, we thus have control over the relative contributions of S_s and S_c to the total signal.

We incorporate nuclear dynamics of the PTS crystal using a multimode Brownian oscillator model [7]. In this model, the nuclear motions in the ground and excited states of the optically active modes are described by multidimensional harmonic oscillators, with mode j being characterized by a fundamental frequency ω_j and a (dimensionless) linear displacement D_j of the equilibrium positions of the ground- and excited-state oscillators. Additionally, each mode is subjected to a damping γ_j and a Gaussian stochastic random force $f_j(t)$ via the Langevin equation. We furthermore model the other nuclear modes of the system collectively using one or more bath coordinates; these bath modes, which are represented by overdamped ($\gamma_i\gg\omega_j$) Brownian oscillators, contribute to the signal by causing line broadening and spectral shifts. The nonlinear response function $R(t_3,t_2,t_1)$ can be calculated exactly for the Brownian oscillator model [7,9]. This mode has previously been applied towards the analysis of pump-probe experiments on solvated dyes [8].

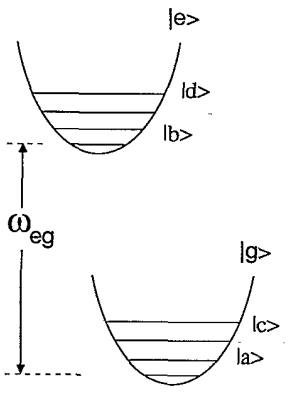

FIG. 1. Displaced oscillator model corresponding to either of the two phonon modes.

Resonance Raman experiments on PTS [1] have identified two phonon modes which are strongly coupled to the excitonic transition, as well as two weaker modes. In the current theoretical treatment, we consider only the two strongly coupled modes, which we model using the vibronic eigenstate representation. These modes, which we shall label α and β, correspond to the C=C and C≡C stretches, respectively, in PTS [1]. We take $\omega_\alpha=1400$ cm^{-1} and $\omega_\beta=2100$ cm^{-1} to be the oscillator fundamental frequencies, with dimensionless displacements $D_\alpha=1.00$ and $D_\beta=0.88$, and no damping, $\gamma_\alpha=\gamma_\beta=0$. We model the bath, which corresponds physically to all of the low-frequency modes of the PTS crystal, using a single overdamped mode in the coordinate representation [7]. We parametrize the overdamped mode by the phonon-bath coupling strength $\Delta\equiv D(\omega k_B T)^{1/2}$, and the bath correlation time scale $\tau_c\equiv\gamma/\omega^2$. In the limit of an inhomogeneously broadened absorption spectrum, we have $\Delta=\Gamma/2.355$, where Γ is the full width at half maximum (FWHM) of the 0-0 absorption line. τ_c is the time scale for the spectral diffusion process; we have $\tau_c=0$ for a homogeneously broadened absorption line, and $\tau_c=\infty$ for the case of purely inhomogeneous broadening. Based on the experimental absorption linewidth [4] and the observed time scale of spectral diffusion (cf. Fig. 3), we use $\Delta=280$ cm^{-1} and $\tau_c=1.3$ ps. In some experiments, Δ may also be obtained from the time-dependent Stokes shift [8]; however, that process is not clearly visible in the experiments presented here, due to the short excited-state lifetime of PTS. We model the pump pulse envelope as a transform-limited Gaussian with full width at half maximum 70 fs, and have included the ≈ 1 ps excited-state lifetime [2] of PTS in the calculation.

In Fig. 2, we display the experimental (left column) and calculated (right column) signals for a resonant pump ($\Omega_p=\omega_{eg}$), at various pump-probe delays. The peaks numbered 1–5 correspond to the resonances at $\omega_T-\omega_{eg}=0$, ω_α, ω_β, $2\omega_\alpha$, and $-\omega_\alpha$, respectively. The strong peaks in Fig. 2 are all negative, corresponding to either a saturated absorption from the ground state (peaks 1–4) or to stimulated emission from the excited to the ground state (peaks 1,5). Peak 5 is not visible in the

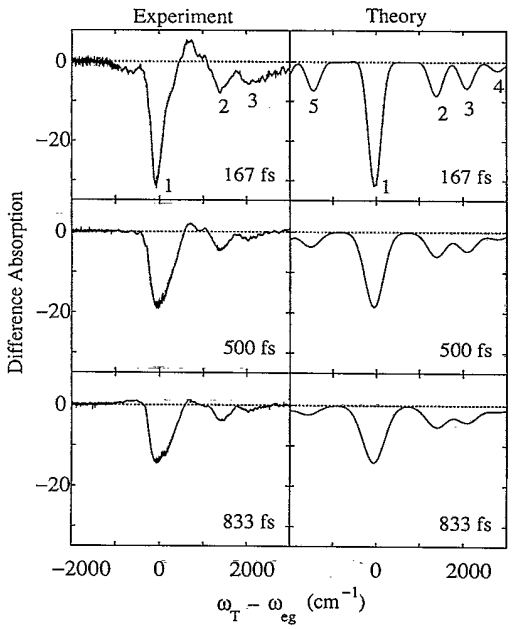

FIG. 2. Experimental and calculated difference absorption line shapes for PTS, at three different τ values, indicated in the frames, with a resonant pump pulse ($\Omega_p = \omega_{eg}$). The experimental signals have been scaled to match the calculated zero-phonon line peak heights. The experimental (calculated) FWHM's for the 0-0 transition are 308 cm^{-1} (382 cm^{-1}), 543 cm^{-1} (524 cm^{-1}), and 558 cm^{-1} (615 cm^{-1}), for $\tau = 167$, 500, and 833 fs, respectively.

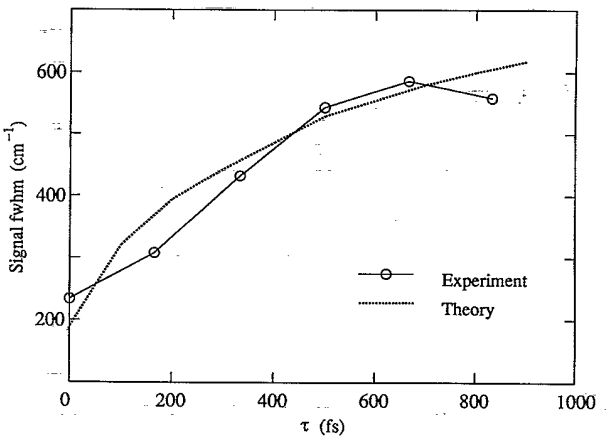

FIG. 3. The full width at half maximum (FWHM) of the 0-0 transition for $\Omega_p = \omega_{eg}$, plotted as a function of the pump-probe relative delay, for the experimental results and for the Brownian oscillator model.

experimental spectra, as the (pump-induced) excited-state population actually absorbs into the conduction band, rather than being emitted back down to the ground state, upon interaction with the probe pulse. This process is not included in our model. Figure 2 shows spectral diffusion, in that the probe difference absorption signal broadens as τ is increased. In Fig. 3, we plot the FWHM of the 0-0 transition versus τ, for six experimental τ values. The dotted curve in the figure gives the FWHM versus τ trend predicted by the Brownian oscillator model. This time-dependent broadening of the signal, which has been observed previously in pump-probe experiments on solvated dyes [11], allows us to determine τ_c, the bath relaxation time scale. It should be noted that the line broadening observed here cannot be adequately described using the Bloch equations, which express the observed linewidths in terms of simple homogeneous and inhomogeneous broadenings; for these experiments, the time dependence of the bath relaxation must be considered explicitly. The experiment shown in Figs. 2 and 3 is essentially a time-resolved hole-burning experiment, and the signal is dominated by $S_s(\omega_T, \Omega_p; \tau)$.

In Fig. 4, we display the experimental (left column) and calculated (right column) signal for several detunings of the pump pulse below the excitonic resonance. When the pump laser is tuned below the excitonic resonance, the signal becomes dominated by $S_c(\omega_T, \Omega_p; \tau)$ and is peaked around $\tau \approx 0$ [cf. Eq. (1b)]; the experimental spectra were taken at the τ value which maximized the signal, and the calculations use $\tau = -10$ fs. In the top frames of Fig. 4, we plot the experimental and calculated spectra for a pump detuning of approximately -1650 cm^{-1}. Agreement of theory and experiment is quite good for $\omega_T - \omega_{eg} < 2000$ cm^{-1} (peaks 1–4). The faint experimental peaks between peaks 2 and 3 and between peaks 3 and 4 are due to the weakly optically active modes not included in the present model. These modes, as well as the proximity of the conduction band, might

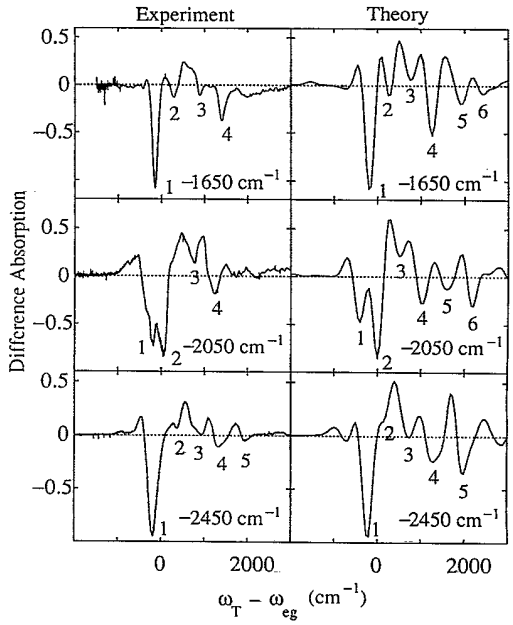

FIG. 4. Experimental and calculated difference absorption line shapes for PTS, with $\tau \approx 0$, at three different pump detunings ($\Omega_p - \omega_{eg}$) from resonance, as indicated. The experimental signals have been scaled to match the calculated peak heights for the strongest peak.

account for the lack of clear experimental signal for $\omega_T - \omega_{eg} > 2000\ \mathrm{cm}^{-1}$.

The resonances in Fig. 4 are caused by the combined effects of resonances in $\omega_T - \omega_{eg}$ in the $\hat{R}_1$ and $\hat{R}_4$ terms of Eq. (1b), and in $\omega_T - \Omega_p$, which arise from the t_2 integration in Eq. (1b). In the top frames of the figure, peaks 1, 2, 4, 5, and 6 are largely due to combinations of $\omega_T - \omega_{eg}$ resonances with 0, 0, ω_α, ω_β, and ω_β, and $\omega_T - \Omega_p$ resonances with ω_α, ω_β, $2\omega_\alpha$, $\omega_\alpha + \omega_\beta$, and $2\omega_\beta$, respectively. Peak 3 is actually caused by interference between two pairs of resonances: $\omega_T - \omega_{eg} \approx 0$ and ω_α; $\omega_T - \Omega_p \approx 2\omega_\alpha$ and ω_β. These contributions can be verified by "turning off" various vibronic levels in the calculation. The present theory thus allows us to ascertain the peak assignments and their relative strengths.

In the middle frames of Fig. 4, we present the experimental and calculated spectra for $\Omega_p \approx \omega_{eg} - 2050\ \mathrm{cm}^{-1}$. The peaks are caused by the same combinations of resonances as in the above spectra, except that in peak 5, the resonances $\omega_T - \omega_{eg} \approx \omega_\alpha$ and $\omega_T - \omega_p \approx 2\omega_\beta$ now also contribute. Peaks 1–4 and 6 are redshifted by 100–150 cm^{-1}, relative to the corresponding peaks in the top frames, and peak 5 (owing to the newly contributing resonances) is redshifted by approximately 225 cm^{-1}. That most of the peaks shift in frequency by an amount less than the shift in Ω_p (200 cm^{-1}) is understandable: Since the peaks are caused by combinations of ω_T and $\omega_T - \Omega_p$ resonances, we expect the observed peaks to redshift by an amount by less than 200 cm^{-1} to remain close to the same $\omega_T - \Omega_p$ resonance, without moving too far from the ω_T resonance. Concomitant with this shift is a difference in the relative peak heights; the transitions corresponding to the two (or more) contributing resonances have different Franck-Condon factors.

In the bottom frames of Fig. 4, we plot the experimental and calculated spectra for a pump detuning of approximately $-2450\ \mathrm{cm}^{-1}$. In this case, peaks 1, 2, 4, and 5 can be attributed to combinations of $\omega_T - \omega_{eg}$ resonances with 0, 0, ω_α, and ω_β, and $\omega_T - \Omega_p$ resonances with ω_β, $2\omega_\alpha$, $\omega_\alpha + \omega_\beta$, and $2\omega_\beta$, respectively. Peak 3 is caused by interference between two pairs of resonances: $\omega_T - \omega_{eg} \approx 0$ and ω_α; $\omega_T - \Omega_p \approx \omega_\alpha + \omega_\beta$ and $2\omega_\alpha$.

In conclusion, we have presented pump-probe difference absorption spectra on PTS with both resonant and nonresonant pump pulses. The resonant data reveal a time-dependent broadening of the difference absorption signal, which may be explained in terms of the relaxation of the crystalline environment ("bath") surrounding the optically active phonon modes. The peaks for nonresonant pumping can be explained in terms of a resonance-enhanced Raman effect; that is, the significant signal comes from the combined effects of Raman resonances and probe absorption resonances. Both kinds of signals, i.e., resonant and nonresonant, are described for the first time by one and the same theory. The quantitative agreement between this theory and the experimental results reinforces the point of view that the near-resonant optical response of polydiacetylene can be completely modeled in terms of the single exciton and its coupling to the lattice.

We wish to thank Dr. M. Thakur for providing the PTS samples. The support of the Air Force Office of Scientific Research and the National Science Foundation is gratefully acknowledged.

[1] D. N. Batchelder and D. Bloor, J. Phys. C **15**, 3005 (1982).
[2] B. I. Greene, J. Orenstein, R. R. Millard, and L. R. Williams, Chem. Phys. Lett. **139**, 381 (1987).
[3] B. I. Greene, J. Orenstein, and L. R. Williams, Phys. Rev. Lett. **58**, 2750 (1987).
[4] B. I. Greene, J. F. Mueller, J. Orenstein, D. H. Rapkine, S. Schmitt-Rink, and M. Thakur, Phys. Rev. Lett. **61**, 325 (1988).
[5] G. J. Blanchard and J. P. Heritage, Chem. Phys. Lett. **177**, 287 (1991).
[6] B. I. Greene, J. Orenstein, and S. Schmitt-Rink, Science **247**, 679 (1990).
[7] Y. J. Yan and S. Mukamel, Phys. Rev. A **41**, 6485 (1990); S. Mukamel, Annu. Rev. Phys. Chem. **41**, 647 (1990).
[8] W. B. Bosma, Y. J. Yan, and S. Mukamel, J. Chem. Phys. **93**, 3863 (1990).
[9] Y. J. Yan and S. Mukamel, in *Recent Trends in Raman Spectroscopy*, edited by S. B. Banerjee and S. S. Jha (World Scientific, Singapore, 1989), p. 160.
[10] S. Saikan, N. Hashimoto, T. Kushida, and K. Namba, J. Chem. Phys. **82**, 5409 (1985).
[11] C. H. Brito Cruz, R. L. Fork, W. H. Knox, and C. V. Shank, Chem. Phys. Lett. **132**, 341 (1986).